# Characterization of tailocins of *Pragia fontium* 24613 and the tailocin loci within the family *Budviciaceae*

Kateřina Snopková [a,b], Eva Chaloupková [a], Matěj Hrala [a], David Šmajs [a,*]

[a] *Department of Biology, Faculty of Medicine, Masaryk University, Kamenice 753/5, 625 00, Brno, Czech Republic*
[b] *Institute for Microbiology, Faculty of Medicine, Masaryk University and St. Anne's University Hospital Brno, Pekařská 664/53, 656 91, Brno, Czech Republic*

## ARTICLE INFO

## ABSTRACT

Tailocins are nano-scale phage tail-like protein complexes that can mediate antagonistic interactions between closely related bacterial species. While the capacity to produce R-type tailocin was found widely across Gammaproteobacteria, the production of F-type tailocins seems comparatively rare. In this study, we examined the freshwater isolate, *Pragia fontium* 24613, which can produce both R- and F-type tailocins. We investigated their inhibition spectrum, focusing on clinically relevant enterobacteria, and identified the associated tailocin gene cluster. Transmission electron microscopy confirmed that inactivation of the tape measure protein within the tailocin cluster disrupted R-tailocin production. Comparative analysis of *Budviciaceae* gene clusters showed high conservation of R-type tailocin genes, whereas F-type tailocin genes were found in only a few species, with little conservation. Our findings indicate a high prevalence of bacteriocin production among underexplored Enterobacteriales species. Detected tailocins showed potential as antimicrobials targeting clinically significant pathogens.

## 1. Introduction

The competition among microorganisms occupying similar ecological niches leads to the production of a wide array of antimicrobial substances. These include type VI secretion system effectors, Rhs proteins, and contact-dependent inhibition proteins which are widely considered to target and kill competitors [1–3]. A class of antibacterial proteins, known as bacteriocins, specifically targets and kills closely related bacterial species [4]. Bacteriocins exhibit considerable diversity in terms of size, genomic localization of their encoding genes, cytotoxic effects, and the spectrum of species they can eliminate [4,5]. Research has shown that bacteriocin production can significantly influence the composition of microbial communities in natural environments [6–8].

Tailocins represent a distinct class of bacteriocins, characterized by large protein complexes that are derived from bacteriophage and which structurally resemble phage tails [9,10]. These nanoscale particles come in two morphologically distinct types: rigid contractile structures (R-type) and flexible, non-contractile particles (F-type). R-type tailocins are thought to be closely related to other contractile injection systems, such as myophage tails [11], Photorhabdus virulence cassettes (PVCs)

[12], Serratia entomophila's antifeeding prophage (Afp) [13], and the Type VI Secretion System [14]. These structures are produced by a wide variety of Gram-negative bacteria [15–19] as well as some Gram-positive species [20,21]. R-type tailocins consist of a rigid tube encased in a contractile sheath, exhibiting six-fold rotational symmetry along their axis [22]. The distal end of the particle contains a baseplate equipped with tail fibers responsible for receptor recognition and initiating sheath contraction [23–25]. The tail tube itself is equipped with a spike protein complex that enables membrane penetration [26]. In contrast, F-type tailocins are less common and have been reported in a limited number of microorganisms, including certain *Pseudomonas* species, *Listeria monocytogenes*, and *Pragia fontium* 24613 [9,27–29]. These particles are flexible, rod-shaped, and feature fiber-like structures on their surface. The F-type pyocin F1, for instance, consists of 23 annular units, measuring a total of 106 nm in length [9]. Only a few bacteria species are known to produce both R- and F-type tailocins [29,30]. Assembly of both types of particles takes place within the bacterial cell, with their release typically following cell autolysis [9,31]. Upon encountering a susceptible bacterium, R-type tailocins induce cell death by depolarizing the cytoplasmic membrane resulting in the collapse of

proton-motive force [32]. However, the mechanism by which F-type tailocins kill target cells remains unclear.

The family *Budviciaceae* comprises Gram-negative, rod-shaped bacteria. Species within this family are found in diverse environments, including freshwater ecosystems (*Pragia fontium, Budvicia aquatica,* and *Limnobaculum parvum*) [33–35], or as part of the gut microbiota of insects and other invertebrates (*Budvicia diplopodorum, Limnobaculum allomyrinae, Limnobaculum eriocheiris,* and *Limnobaculum xujianqingii*) [36–38]. Additionally, certain species inhabit warm-blooded animals, such as *Limnobaculum zhutongyuii* [38,39], and humans, represented by *Leminorella grimontii* and *Leminorella richardii* [40]. Despite their various habitats, their pathogenicity remains largely unknown. Production of phage tail-like inhibition agents has been documented in several strains of *Pragia* and *Budvicia* [41]. The majority of tailocin-producing strains are known to synthesize R-type particles. Notably, only one strain, *P. fontium* 24613, is capable of producing both R- and F-type tailocins [29]. The pore-forming activity of these tailocins was characterized using both living cells and *in vitro* model membranes [42].

This study focuses on identifying the genetic clusters encoding tailocins in *P. fontium* 24613, assessing the inhibitory spectrum of this strain, and comparing tailocin gene clusters among closely related strains within the *Budviciaceae* family.

## 2. Material and methods

### 2.1. Bacterial strains and growth conditions

*P. fontium* 24613 (tailocin producer) was used throughout this study. The antagonistic activity of *P. fontium* 24613 was assessed against *P. fontium* 24647 (indicator strain) and related strains from the family *Budviciaceae, Yersiniaceae, Pectobacteriaceae, Morganellaceae, Enterobacteriaceae,* and the genus *Plesiomonas* (a list of strains is shown in Table S1). All strains are deposited in the collection of the Department of Biology, Masaryk University, Brno, or the Czech Collection of Microorganisms, Brno, Czech Republic. Bacteria were grown on TY agar (8 g l$^{-1}$ casein, 5 g l$^{-1}$ yeast extract, 5 g l$^{-1}$ sodium chloride, 8 g l$^{-1}$, pH 7.5; all Hi-Media, Mumbai, India).

### 2.2. Bacteriocin assay

The inhibition spectrum of *P. fontium* 24613 was determined using an overlay plate assay technique [43]. Briefly, strain 24613 was inoculated on TY agar supplemented with mitomycin C (final concentration 0.5 μg ml$^{-1}$) and cultivated at 25 °C for 48 h. Colony of the producer strain was killed by chloroform vapors and overlayed with soft TY medium (0.6% of agar) containing 10$^8$ CFU/ml of the indicator strain. Plates were incubated at 30 °C for 48 h. A clear zone of growth inhibition around the producer was assessed. No plaques were detected at the edges of this inhibition zone or elsewhere on the cultivation plates, suggesting that the inhibitory effect was without signs of phage lysis.

The crude bacteriocin was prepared for subsequent dilution assays as follows. An overnight culture (5 ml) of *P. fontium* 24613 was grown in TY broth at 25 °C and 200 rpm. The culture was then diluted 1:10 with fresh TY broth and incubated at 25 °C and 200 rpm until the culture reached an OD$_{600}$ of 0.9. Mitomycin C was added to a final concentration of 0.5 μg ml$^{-1}$, and the culture was incubated for an additional 4 h. The culture was then centrifuged at 5000 rpm, and the cell-free supernatant was collected. To ensure sterility, the supernatant was exposed to chloroform vapors for 1 h. The resulting cell-free supernatant was serially diluted and used for inhibition assays against indicator strain *P. fontium* 24647 on agar plates as described above.

### 2.3. Genomic inspection of the tailocins gene cluster in P. fontium 24613

The genome of *P. fontium* 24613 (GenBank acc. no. CP010423.1) was inserted into the PHASTER, https://phaster.ca [44]. (Pro)phage clusters

were manually re-annotated, and the putative tailocin cluster was identified. BPROM software, http://linux1.softberry.com/berry.phtml, was used to identify the putative promoters and Lex A binding motifs in the tailocin gene cluster. Average nucleotide identity (ANI) between tailocins of *P. fontium* 24613 and relevant phages was calculated using the EzBioCloud server http://www.ezbiocloud.net/tools/ani [45].

### 2.4. Chromosomal mutagenesis of P. fontium 24613

Random insertion mutagenesis using mini-Tn10 transposons was performed to identify the genome location of the tailocin gene cluster. Suicide-plasmid NKBOR, carrying a mini-Tn10 transposon (2.4 kb; kanamycin resistance), was electroporated into *P. fontium* 24613 cells [46]. Transformants were selected on TY agar supplemented with kanamycin (final concentration 0.05 g l$^{-1}$, Sigma-Aldrich, St. Louis, USA). Overlay plate assays, using indicator strain *P. fontium* 24647 harboring pCR2.1-TOPO (ThermoFisher Scientific; Waltham, USA; kanamycin resistance), were used to detect independent inhibition-deficient mutants. Genomic DNA of mutants 29 1G and 72 9G was extracted using the phenol-chloroform protocol and digested with *Bgl*II and *Nhe*I, respectively. Fragments were self-ligated with T4 DNA ligase (ThermoFisher Scientific; Waltham, USA) and used as a template for inverse PCR reactions. Regions flanking the mini-Tn10 transposon were amplified using GeneAmp® XL PCR Kit (ThermoFisher Scientific; Waltham, USA) and NKBORout_3: 5′-AACAGCCAGGGATGTAACG-3′ and NKBORout_4: 5′-GCAGGGCTTTATTGATCCA-3′primers [47]. PCR products were sequenced using GATC Biotech (Constance, Germany) and aligned to the *P. fontium* 24613 genome using SeqMan software (DNASTAR, Madison, USA).

### 2.5. Large-scale production and purification of P. fontium 24613 tailocins

Fifty microliters of overnight *P. fontium* 24613 culture and mutants 29 1G and 72 9G were used as an inoculum for a culture cultivated at 30 °C in 100 ml of TY medium until it reached an OD$_{600}$ equal to 0.5. Subsequently, mitomycin C was added at a final concentration of 0.5 μg ml$^{-1}$, and cultivation continued for 3 h. Samples were then treated according to phage protocols [48]. Briefly, NaCl (at a final concentration of 0.5 M) was added for 1 h to dissolve particles on the bacterial cells, and the debris was collected using centrifugation at 14,000 g for 15 min. Subsequently, polyethylene glycol 8000 (at a final concentration of 10% w/v; Sigma-Aldrich, St. Louis, USA) was added to the supernatant. Phage tail-like particles were precipitated overnight at 4 °C and collected using centrifugation at 8000 g for 1 h at 4 °C. The pellet was resuspended in 2 ml of SM buffer (100 mM NaCl, 8 mM MgSO$_4$·7H$_2$O, 50 mM Tris-Cl), and the solution was applied to a CsCl gradient (1.45–1.7 g ml$^{-1}$) and centrifuged (87,000 g at 10 °C for 2 h). The collected tailocin fraction was dialyzed against SM buffer overnight.

### 2.6. Dark-field transmission electron microscopy

Purified tailocins (5 μl) from (i) wild type *P. fontium* 24613 and (ii) transposon mutants 29 1G and 72 9G were applied to glow discharge-activated carbon-coated copper grids (Pyser–SGI, Edenbridge, United Kingdom). Negative staining was performed using 2% (w/v) ammonium molybdate for 10–30 s, and tailocins were visualized using a MORGAGNI 268D microscope (FEI, Hillsboro, USA). The dimensions of the particles were analyzed using ImageJ [49].

### 2.7. Comparison of the tailocin loci within the family Budviciaceae

Publicly available genomes across the family *Budviciaceae* were compared in the Gene Ortholog Neighborhood Viewer at the Integrated Microbial Genomes website, https://img.jgi.doe.gov/. Predicted amino acid sequences of the *P. fontium* 24613 R-tailocin sheath (GenBank acc.

no. QQ39_04820) and tube protein sequences (acc. no. QQ39_04825) were used as queries. The default parameters of bidirectional blast analyses were used. The identified phage-tail-related gene clusters were manually curated and re-annotated using results from PHASTER, https://phaster.ca [44], SMART, http://smart.embl-heidelberg.de/, and InterPro, https://www.ebi.ac.uk/interpro, analyses. Genomes of *Budviciaceae* members containing homologs of the sheath and tube proteins were further analyzed, *i.e.*, *P. fontium* DSM 5563ᵀ (GenBank ac. no. GCA_900112475.1), *P. fontium* NCTC 12284 (GCA_900454805.1), *P. fontium* NCTC 12285 (GCA_900638655.1), *B. aquatica* DSM 5075ᵀ (GCA_000427805.1), *L. grimontii* ATCC 33999ᵀ (GCA_000439085.1), *L. richardii* NCTC 12151ᵀ (GCA_900478135.1), *L. parvum* HYN0051ᵀ (GCA_003096015.2), *L. zhutongyuii* CF-458ᵀ (GCA_004295645.1), and *L. zhutongyuii* CF-917 (GCA_006964055.1). The genomes of *B. diplopodorum* D9 (GCA_009800925.1), *L. xujianqingii* CF-1111 (GCA_013394855.1), and *L. allomyrinae* BWR-B9 (GCA_016649425.1) lacked the phage sheath and tube protein homologs (QQ39_04820 and QQ39_04825) and were discarded from further analysis.

## 3. Results

### 3.1. Strain-specific inhibitory activity of Pragia fontium 24613

Antagonistic interactions of *P. fontium* 24613 were assessed against related enterobacteria (order *Enterobacterales*) using the overlay plate assays. Results revealed only narrow inhibition zones (<2 mm), which suggested the production of large, slowly diffusing inhibitory protein complexes such as tailocins [49,50]. No phage plaques were detected during the overlay plate assay. The undiluted and 10-fold diluted crude extract of the producer strain inhibited the indicator strain *P. fontium* 24647 with no plaques observed.

The inhibition spectrum included one *P. fontium* strain (1/5; 20.0%), five *B. aquatica* (5/9; 55.6%), five *Yersinia enterocolitica* (5/5; 100.0%), two *Yersinia kristensenii* (2/5; 40.0%), two *Yersinia aldovae* (2/5; 40.0%), one *Yersinia frederiksenii* (1/5; 20.0%), and one *Escherichia coli* strain (1/18; 5.6%), see Fig. 1. The remaining strains from the order

*Enterobacterales* (namely *L. grimontii, Xenorhabdus* spp.*, Photorhabdus* spp.*, Moellerella* spp.*, Morganella* spp.*, Providencia* spp.*, Proteus* spp.*, Plesiomonas shigelloides*) were non-susceptible.

### 3.2. Genomic insights into bacteriocin production of Pragia fontium 24613

The genomic location of the *P. fontium* 24613 tailocins gene cluster was identified based on *in silico* genome analysis using a (pro)phage finder tool. The gene cluster of interest contained both siphophage and myophage tail homologs (QQ39_04725–04905, total of 37 genes, 32.0 kb). The cluster was found localized between genes encoding multidrug resistance proteins A and B and has a lower GC content (42.0% vs. 45.4% of the whole genome). A deeper, manual analysis revealed the typical signs of a tailocin cluster: (i) phage tail homologs only (no genes for head formation, nucleic acid replication, and packaging), (ii) a regulatory region containing Cro/cI phage repressor and promoter sequences with a LexA binding motif, and (iii) the presence of lytic cassettes consisting of holin and endolysin genes.

### 3.3. F- and R-type tailocin gene cluster in Pragia fontium 24613

The regulatory region (QQ39_04725–04730) and the lytic cassette (QQ39_04735–04745) were located at the proximal end, whereas the structural genes were found downstream, see Fig. 2. The F-type tailocin locus contained 13 genes (QQ39_04750–04810; 42.0% of the total cluster length) that encoded all structural components of siphophage tails, *i.e.*, major tail proteins, minor tail proteins, tape measure proteins (TMP), host specificity proteins, tail assembly chaperones, and tail fiber proteins. The majority of the genes (except for genes encoding tail fiber proteins) exhibited homology with the T1 siphophage (GenBank acc. no. NC_005833.1, genes T1p32–41), with the nucleotide sequence identity exceeding 52%. R-type tailocin genes were located more downstream, at the distal end of the gene cluster, and contained 19 genes (QQ39_04815–04905; 47.2% of the total cluster length). The R-specific locus encoded homologs of the tube and sheath proteins, TMP, baseplate
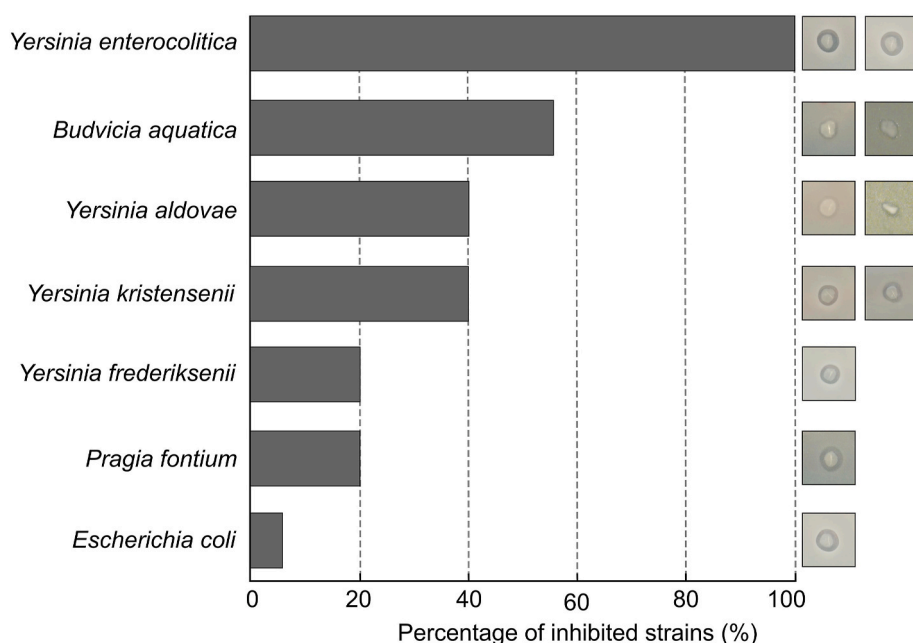


**Fig. 1.** Growth inhibition caused by *P. fontium* 24613 on bacterial strains of *Enterobacterales*
*P. fontium* 24613 antagonized species from the family *Budviciaceae* including one *P. fontium* strain (1/5; 20.0%), five *Budvicia aquatica* strains (5/9; 55.6%), strains from the family *Yersiniaceae* including five *Yersinia enterocolitica* (5/5; 100.0%), two *Yersinia kristensenii* (2/5; 40.0%), two *Yersinia aldovae* (2/5; 40.0%), and one *Yersinia frederiksenii* strain (1/5; 20.0%), and strains of *Enterobacteriaceae* including one *Escherichia coli* strain (1/21; 4.8%). Representative inhibition zones for each species are displayed. Only species with inhibited strains are shown.
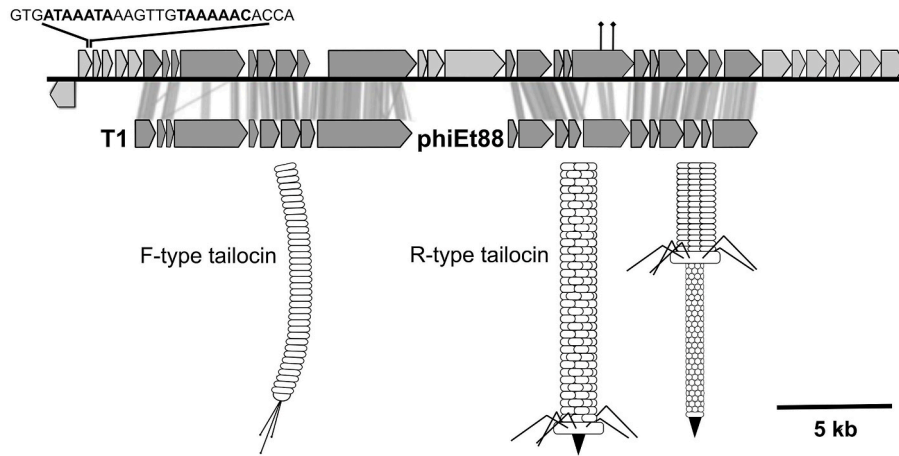
**Fig. 2.** F- and R-type tailocin gene cluster in *P. fontium* 24613

The tailocins cluster (QQ39_04725–04905) contained regulatory region (QQ39_04725–04730) with two LexA binding motifs (sequences shown in bold), lytic cassette genes (QQ39_04735–04745), F-specific genes (QQ39_04750–04810), and R-specific genes (QQ39_04815–04905). A schematic visualization of F- and R-type tailocin is below. Genes homologous to siphophage T1 (T1p32–41) and myophage phiEt88 (P88_00130–00230) are dark grey. Diamonds indicate positions of mini-Tn10 transposon insertions. The size marker represents 5 kb.

proteins, tail fiber proteins, and tail fiber assembly chaperones. The structural genes (except for tail fiber proteins and fiber assembly chaperones) were very similar to the phiEt88 myophage (acc. no. NC_015295.1, genes P88_00130–00230), with the nucleotide identity of 54–72%. The annotation of all genes in the cluster is listed in Table S2.

### 3.4. Confirmation of the Pragia fontium 24613 tailocin gene function
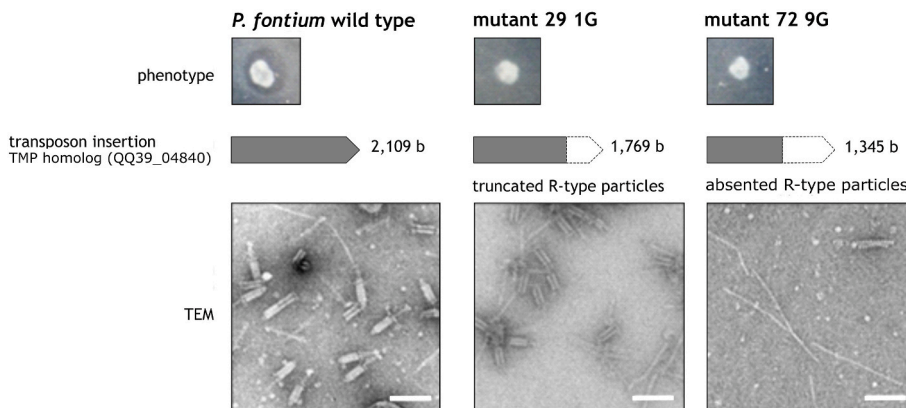
Transposon-inactivation assays were used to confirm the tailocin locus. During overlay plate assays, two independent mutants (29 1G and 72 9G) out of the 7,872 analyzed led to a complete loss of inhibition zones. Both transposon insertions were located in the TMP homolog (QQ39_04840) inside the presumed tailocin cluster. Mutant 72 9G contained the transposon at coordinate 1,345, whereas mutant 29 1G contained the transposon at coordinate 1,769 out of 2,109 b. Both mutants exhibited no inhibitory activity against any of the originally susceptible strains, including *P. fontium*, *B. aquatica*, *E. coli* and *Yersinia* spp.

Transmission electron microscopy (TEM) of the *P. fontium* 24613 wildtype confirmed the presence of R- and F-type particles; however, no full phages were detected. R tailocins had a typical morphology, *i.e.*, an inner tube encompassed by a contractile outer sheath. All conformations of R tailocins were detected; relaxed full-length particles (length 112.4 $\pm$ 4.3 nm, based on measurements of 10 particles), contracted particles (length 41.8 $\pm$ 1.5, based on 8 particles), and empty contracted sheaths (length 41.2 $\pm$ 2.0 nm, based on 20 particles). The F-type tailocins were detected less frequently, and their dimensions were not measured due to their irregular shape. Transposon-inactivated mutants affected the production of R-type tailocins (Fig. 3); in mutant 72 9G (transposon inserted at position 1,345 of 2,109 b), there was a complete loss of R tailocin production while mutant 29 1G, with the insertion closer to the distal end (1,769 of 2,109 b) produced truncated particles (contracted sheath length was 37.0 $\pm$ 1.3 nm vs. 41.2 $\pm$ 2.0 nm in the wild type; no relaxed particles of mutants were detected in TEM).

### 3.5. Tailocin gene clusters among Budviciaceae

We analyzed genomes from 13 members of the *Budviciaceae* family. The genomes of *P. fontium* 24613, DSM 5563[T], NCTC 12284, NCTC 12285, *B. aquatica* DSM 5075[T], *L. grimnotii* ATCC 33999[T], *L. richardii* NCTC 12151, *L. parvum* HYN0051[T], *L. zhutongyuii* CF-917, and CF-458[T] contained at least one tailocin cluster. *In silico* gene mining revealed that the locus encoding both R- and F-type particles were localized in the genome of *P. fontium* 24613 and *B. aquatica* DSM 5075[T], whereas only the R tailocin cluster (*i.e.*, not accompanied by a F-specific gene cluster)



**Fig. 3.** Transposon-inactivation assay confirming the *P. fontium* 24613 tailocin locus

Abbreviation: TEM, transmission electron microscopy; TMP, tape measure protein. Transposon insertion into TMP (QQ39_04840) led to (i) truncation of R particles (mutant 29 1G; insertion at 1,769 of 2,109 b) or (ii) undetectable R particle production (mutant 72 9G; insertion at 1,345 of 2,109 b). The size marker indicates 100 nm.

was detected in other *P. fontium* strains, *Leminorella* spp., *L. parvum* and *L. zhutongyuii* (Fig. 4). All gene clusters were located within the multi-drug efflux system homologs. The strong overall synteny could be seen in the first four genes encoding Cro/CI repressor (Pfam PF01381 and PF00717), phage antitermination protein Q (PF06530), holin (PF16083), and phage lysozyme (PF 00959), which were conserved across all genomes. The lytic cassette module of *P. fontium* NCTC 12284 and *Leminorella* spp. contained both Rz and Rz1 "Siam twin" genes (*i.e.*, genes sharing the same locus but using different reading frames); in the rest of the genomes, only Rz1 gene homologs were found. The locus between the lytic cassette and R-specific genes was the most variable region; in *P. fontium* 24613 and *B. aquatica* DSM 5075$^T$, the F-specific genes were present, in the genomes of *Limnobaculum* spp., tailocin non-related genes were detected in this region (the only exception was the presence of tail fiber protein homologs); in *Leminorella* spp. and other *P. fontium* strains, this part of the gene cluster was completely missing.

## 4. Discussion

Tailocins represent a group of highly specialized tail-like antibacterial protein complexes derived from lysogenic phages [10,28]. Tailocins have been recently considered as an alternative to commercial antibiotics because of their high specificity and minimal side effects [17,27,51,52]. Production of narrow-spectrum particles by several *Pragia* and *Budvicia* strains was first observed by Šmarda and Benada [29], but at that time, no antagonistic assay against clinically relevant enterobacteria was performed. In this study, we assessed the inhibitory activity of the *P. fontium* 24613 strain against several species of *Enterobacterales*. *P. fontium* 24613 antagonized 17 strains (17.7%), including several *Yersinia* species. Based on the inhibitory spectrum of *P. fontium* 24613, tailocin particles could be considered as antimicrobial agents against *Y. enterocolitica* infections since all tested strains were susceptible. However, a limited number *Y. enterocolitica* strains were tested and therefore verification of the inhibition effect should be performed with the wider *Y. enterocolitica* collection.

Our study detected genes responsible for both R- and F-type tailocins produced by *P. fontium* 24613. In contrast to the pyocin R/F clusters found in *Pseudomonas* spp., the F-specific region was located upstream of the R-specific genes. The size of tailocin clusters varied significantly between species due to, *e.g.*, the presence of cargo genes or variable numbers of tail fiber gene homologs. Furthermore, the size of the *P. fontium* 24613 locus (32 kb in length) is closer to double tailocin producers including *Pseudomonas aeruginosa* PAO1 (26 kb [9]), *Pseudomonas chlororaphis* 30–84 (34 kb [8]) or *Pseudomonas fluorescens* SF4c (39 kb [53]), and larger than single tailocin clusters identified in other *Budviciaceae* genomes (18–25 kb), *Pseudomonas putida* RW10S2 (19 kb [54]), *Stenotrophomonas maltophilia* (19 kb [15]), *Kosakonia radicincitans* DMS 16656 (21 kb [10]) or *Burkholderia cenocepacia* BC0425 (23 kb [55]).

Simultaneous production of two or more tailocin types is quite rare; although single R-type tailocin production was observed for various species, including *Serratia proteamaculans* [17], *Pectobacterium carotovorum* [56], *Y. enterocolitica* [57], and *Clostridioides difficile* [20]. The clinically relevant *Pseudomonas* genus can synthetize various combinations of tailocin types; *P. aeruginosa* HB15 or BL03 harbor genes for R-type tailocins only [5], *P. aeruginosa* PML14 secrete only F-type pyocins [30], whereas *P. aeruginosa* PAO1 or *P. fluorescens* SF4c synthesize both particle types [30,53], and finally, *P. chlororaphis* 30-84 and *P. protegens* CHA0 produce two R tailocins [8,58]. If a strain harbors genes for more than one tailocins, their target spectra were different [30,59,60].

Part of the tailocin gene cluster was conserved among the majority of analyzed *Budviciaceae* genomes and included R-specific genes encoding tail sheaths (DUF3383), tubes (DUF3277), base plates, TMP, and tail fiber proteins. While the upstream genes (*i.e.*, genes encoding tail tubes, sheaths, and base plate proteins) belong to the most conserved genes, striking differences were found in the distal part of the cluster, mainly in the number of genes encoding tail fiber and tail fiber assembly chaperones (which varies in number from two in *B. aquatica* DSM 5075$^T$ to six in *P. fontium* NCTC 12285 and *L. richardii* NCTC 12151), or the presence of genes for transferase or site-specific DNA recombinase homolog (Fig. 5).

On the other hand, F-specific genes were detected in only two genomes, in *P. fontium* 24613 and in *B. aquatica* DSM 5075$^T$. Both F-regions contained all major components for particle assembly (*i.e.*, homologs of minor and major tail proteins, host specificity proteins,
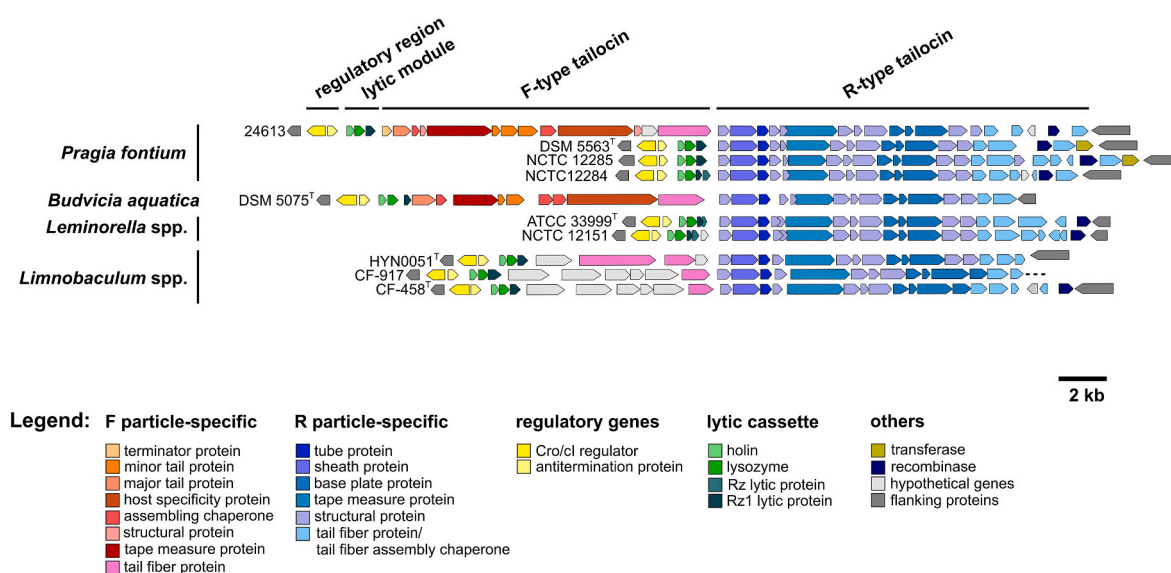


**Fig. 4.** Tailocins gene clusters across the family *Budviciaceae*
R-type tailocin genes are shown in orange and red, F-specific genes in blue, regulatory genes in yellow, lysis-related genes in green, and other genes in grey. Genes for R-type particles were found in all shown genomes, whereas F-tailocin genes were only found in the genomes of *P. fontium* 24613 and *B. aquatica* DSM 5075$^T$. All genomes were obtained from the GenBank database; accession numbers are listed in the Material and methods section. The tailocin gene cluster of *L. zhutongyuii* CF-917 was found interrupted, likely due to the draft character of the genome sequence. The scale bar indicates 2 kb. (For interpretation of the references to color in this figure legend, the reader is referred to the Web version of this article.)
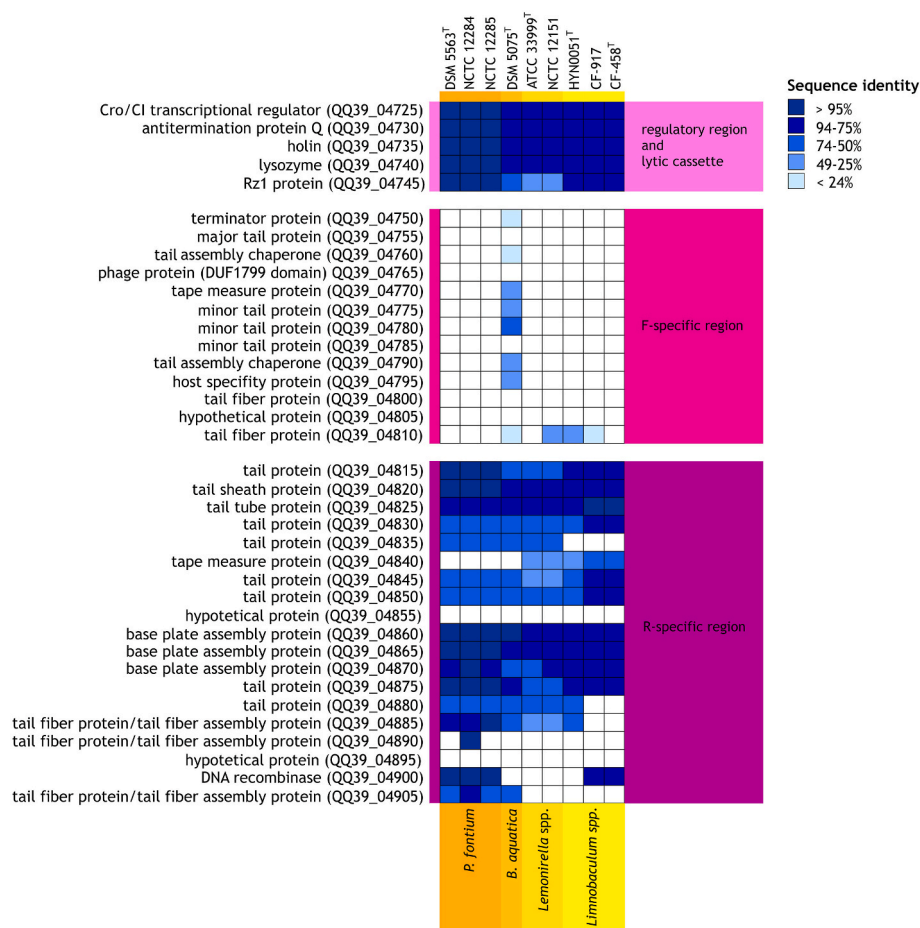
**Fig. 5.** Protein sequence identities among tailocin clusters in the family *Budviciaceae*

The degree of amino acid identity is visualized by the shade of blue color, where deeper color boxes represent greater identity. Genes encoding lytic cassette products, tail tubes, tail sheaths, and base plates of R-type tailocins were the most conserved across the characterized genomes. All sequences were obtained from the GenBank database; accession numbers are listed in the Material and methods section. (For interpretation of the references to color in this figure legend, the reader is referred to the Web version of this article.)

TMP, and tail fiber proteins) with a relatively conserved order. However, protein identity between corresponding genes was very low (20–35% for the majority of proteins), and several genes were missing in strain DSM 5075[T].

Production of R-type tailocins by *P. fontium* 24613 was disrupted by transposon insertions into the gene that encodes TMP. Mutants with defective F-tailocin production were not detected in our study; however, they are easily overlooked during library screening because of the lower inhibition capacity of F-type fonticins (300 F-pyocins but only 1–2 R-pyocins can kill sensitive *Pseudomonas* spp. cells; [9]) and the simultaneous production of R-type tailocins. It has been previously shown that the TMP is essential for the assembly of phage tails and phage tail-like structures (*e.g.*, tailocins, Type III and VI Secretion Systems) because it determines structure length [60,61]. Deletions or duplications of TMP genes lead to proportionally shorter or longer structures [62–64]. Moreover, TMP gene deletion resulted in the abortion of tailocin secretion in *P. fluorescens* SF4c [65]. Rybakova and colleagues [64] proposed a correlation between the TMP gene and particle length, including a prediction of the minimal gene length needed to maintain function. We speculate that in mutant 29 1G (transposon insertion in 1, 769 of 2,109 b), TMP gene function was partially maintained because we observed truncated R particles, whereas in mutant 72 9G (transposon insertion in 1,345 of 2,109 b), the TMP gene was disrupted and no R-particles were found.

A common ancestor for prophages and tailocins was proposed for several particles, such as various R-pyocins [54], F-pyocin of

*P. aeruginosa* PAO1 [30], or R-tailocin produced by *Pectobacterium carotovorum* subsp. *carotovorum* Er [57]. Horizontal gene transfer of the tailocin cluster likely occurred independently in different species [66]. Due to the high gene synteny across R-tailocin genes in *Budviciaceae* genomes, we can speculate that the locus was obtained from phage phi*Et88* (infecting *Erwinia tasmaniensis*) followed by subsequent modifications of the gene cluster. We found high similarity between the F-type tailocin of *P. fontium* 24613 and the lysogenic phage T1 and between the F-type aquaticin of *B. aquatica* DSM 5075[T] and the lambdoid phage Gifsy-2. The different origins of both F-specific genes, together with the absence of F-type genes in other *P. fontium* and *B. aquatica* strains [29], support the hypothesis that genes encoding F-particles were obtained independently, strain specifically, and from different source organisms.

## Conclusion

Tailocins represent a promising class of antimicrobial agents with a high specificity. This study identified and characterized a tailocin gene cluster in *P. fontium* 24613, along with similar clusters in other species within the *Budviciaceae* family. Our findings underscore the potential of *Budviciaceae* to produce these particles, particularly R-type tailocins. Moreover, we discovered genes encoding the less common F-type tailocins in the genomes of *P. fontium* 24613 and *B. aquatica* DSM 5056[T]. Importantly, the tailocins produced by *P. fontium* 24613 were shown to effectively inhibit the growth of clinically significant enterobacteria,

including *Yersinia enterocolitica*.

## Declaration of generative AI and AI-assisted technologies in the writing process

During the preparation of this work the authors used ChatGPT (version GPT-4) in order to improve language and readability. After using this tool/service, the authors reviewed and edited the content as needed and take full responsibility for the content of the publication.

## Funding information

## CRediT authorship contribution statement

**Kateřina Snopková:** Writing – review & editing, Writing – original draft, Visualization, Methodology, Investigation, Data curation, Conceptualization. **Eva Chaloupková:** Writing – review & editing, Investigation. **Matěj Hrala:** Writing – review & editing, Methodology, Investigation. **David Šmajs:** Writing – review & editing, Supervision, Formal analysis.

## Acknowledgements

## Appendix A. Supplementary data

Supplementary data to this article can be found online at https://doi.org/10.1016/j.resmic.2024.104261.

## References

[1] Braun V, Patzer SI. Intercellular communication by related bacterial protein toxins: colicins, contact-dependent inhibitors, and proteins exported by the type VI secretion system. FEMS Microbiol Lett 2013;345:13–21. https://doi.org/10.1111/1574-6968.12180.

[2] Ruhe ZC, Wallace AB, Low DA, Hayes CS. Receptor polymorphism restricts contact-dependent growth inhibition to members of the same species. mBio 2013;4: e00480. https://doi.org/10.1128/mBio.00480-13. 13.

[3] Russell AB, LeRoux M, Hathazi K, Agnello DM, Ishikawa T, Wiggins PA, et al. Diverse type VI secretion phospholipases are functionally plastic antibacterial effectors. Nature 2013;496:508–12. https://doi.org/10.1038/nature12074.

[4] Cascales E, Buchanan SK, Duché D, Kleanthous C, Lloubès R, Postle K, et al. Colicin biology. Microbiol Mol Biol Rev 2007;71:158–229. https://doi.org/10.1128/MMBR.00036-06.

[5] Ghequire MGK, De Mot R. Ribosomally encoded antibacterial proteins and peptides from Pseudomonas. FEMS Microbiol Rev 2014;38:523–68. https://doi.org/10.1111/1574-6976.12079.

[6] Bruce JB, West SA, Griffin AS. Bacteriocins and the assembly of natural *Pseudomonas fluorescens* populations. J Evol Biol 2017;30:352–60. https://doi.org/10.1111/jeb.13010.

[7] Granato ET, Meiller-Legrand TA, Foster KR. The evolution and ecology of bacterial warfare. Curr Biol 2019;29:R521–37. https://doi.org/10.1016/j.cub.2019.04.024.

[8] Dorosky RJ, Pierson LS, Pierson EA. Pseudomonas chlororaphis produces multiple R-tailocin particles that broaden the killing spectrum and contribute to persistence in rhizosphere communities. Appl Environ Microbiol 2018;84:e01230. https://doi.org/10.1128/AEM.01230-18. 18.

[9] Michel-Briand Y, Baysse C. The pyocins of *Pseudomonas aeruginosa*. Biochimie 2002;84:499–510. https://doi.org/10.1016/s0300-9084(02)01422-0.

[10] Patz S, Becker Y, Richert-Pöggeler K, Berger B, Ruppel S, Huson D, et al. Phage tail-like particles are versatile bacterial nanomachines - a mini-review. J Adv Res 2019; 19. https://doi.org/10.1016/j.jare.2019.04.003.

[11] Leiman PG, Basler M, Ramagopal UA, Bonanno JB, Sauder JM, Pukatzki S, et al. Type VI secretion apparatus and phage tail-associated protein complexes share a common evolutionary origin, vol. 106. Proceedings of the National Academy of Sciences; 2009. p. 4154–9. https://doi.org/10.1073/pnas.0813360106.

[12] Jiang F, Li N, Wang X, Cheng J, Huang Y, Yang Y, et al. Cryo-EM structure and assembly of an extracellular contractile injection system. Cell 2019;177:370–383. e15. https://doi.org/10.1016/j.cell.2019.02.020.

[13] Hurst MRH, Glare TR, Jackson TA. Cloning *Serratia entomophila* antifeeding genes-a putative defective prophage active against the grass grub *Costelytra zealandica*. J Bacteriol 2004;186:5116–28. https://doi.org/10.1128/JB.186.15.5116-5128.2004.

[14] Basler M, Pilhofer M, Henderson GP, Jensen GJ, Mekalanos JJ. Type VI secretion requires a dynamic contractile phage tail-like structure. Nature 2012;483:182–6. https://doi.org/10.1038/nature10846.

[15] Liu J, Chen P, Zheng C, Huang Y-P. Characterization of maltocin P28, a novel phage tail-like bacteriocin from *Stenotrophomonas maltophilia*. Appl Environ Microbiol 2013;79:5593–600. https://doi.org/10.1128/AEM.01648-13.

[16] Ghequire MGK, De Mot R. The tailocin tale: peeling off phage tails. Trends Microbiol 2015;23:587–90. https://doi.org/10.1016/j.tim.2015.07.011.

[17] Jabrane A, Sabri A, Compère P, Jacques P, Vandenberghe I, Van Beeumen J, et al. Characterization of serracin P, a phage-tail-like bacteriocin, and its activity against *Erwinia amylovora*, the fire blight pathogen. Appl Environ Microbiol 2002;68: 5704–10. https://doi.org/10.1128/AEM.68.11.5704-5710.2002.

[18] Strauch E, Kaspar H, Schaudinn C, Dersch P, Madela K, Gewinner C, et al. Characterization of enterocoliticin, a phage tail-like bacteriocin, and its effect on pathogenic *Yersinia enterocolitica* strains. Appl Environ Microbiol 2001;67: 5634–42. https://doi.org/10.1128/AEM.67.12.5634-5642.2001.

[19] Nguyen AH, Tomita T, Hirota M, Sato T, Kamio Y. A simple purification method and morphology and component analyses for carotovoricin Er, a phage-tail-like bacteriocin from the plant pathogen *Erwinia carotovora* Er. Biosci Biotechnol Biochem 1999;3:1360–99. https://doi.org/10.1271/bbb.63.1360.

[20] Gebhart D, Williams SR, Bishop-Lilly KA, Govoni GR, Willner KM, Butani A, et al. Novel high-molecular-weight, R-type bacteriocins of *Clostridium difficile*. J Bacteriol 2012;194:6240–7. https://doi.org/10.1128/JB.01272-12.

[21] Kamoun F, Fguira IB, Tounsi A, Abdelkefi-Mesrati L, Sanchis V, Lereclus D, et al. Generation of Mini-Tn10 transposon insertion mutant library of *Bacillus thuringiensis* for the investigation of genes required for its bacteriocin production. FEMS Microbiol Lett 2009;294:141–9. https://doi.org/10.1111/j.1574-6968.2009.01559.x.

[22] Ge P, Scholl D, Leiman PG, Yu X, Miller JF, Zhou ZH. Atomic structures of a bactericidal contractile nanotube in its pre- and postcontraction states. Nat Struct Mol Biol 2015;22:377–82. https://doi.org/10.1038/nsmb.2995.

[23] Kurosawa Y, Ikeda K, Egami F. Destruction of the receptor susbtance for pyocin by a liver extract of *Turbo cornutus*. J Gen Appl Microbiol 1973;19:375–83. https://doi.org/10.2323/jgam.19.375.

[24] Köhler T, Donner V, van Delden C. Lipopolysaccharide as shield and receptor for R-pyocin-mediated killing in *Pseudomonas aeruginosa*. J Bacteriol 2010;192:1921–8. https://doi.org/10.1128/JB.01459-09.

[25] Buth SA, Shneider MM, Scholl D, Leiman PG. Structure and analysis of R1 and R2 pyocin receptor-binding fibers. Viruses 2018;10:427. https://doi.org/10.3390/v10080427.

[26] Browning C, Shneider MM, Bowman VD, Schwarzer D, Leiman PG. Phage pierces the host cell membrane with the iron-loaded spike. Structure 2012;20:326–39. https://doi.org/10.1016/j.str.2011.12.009.

[27] Blasco L, de Aledo MG, Ortiz-Cartagena C, Blériot I, Pacios O, López M, et al. Study of 32 new phage tail-like bacteriocins (pyocins) from a clinical collection of *Pseudomonas aeruginosa* and of their potential use as typing markers and antimicrobial agents. Sci Rep 2023;13:117. https://doi.org/10.1038/s41598-022-27341-1.

[28] Lee G, Chakraborty U, Gebhart D, Govoni GR, Zhou ZH, Scholl D. F-type bacteriocins of Listeria monocytogenes: a new class of phage tail-like structures reveals broad parallel coevolution between tailed bacteriophages and high-molecular-weight bacteriocins. J Bacteriol 2016;198:2784–93. https://doi.org/10.1128/JB.00489-16.

[29] Smarda J, Benada O. Phage tail-like (high-molecular-weight) bacteriocins of *Budvicia aquatica* and *Pragia fontium* (*Enterobacteriaceae*). Appl Environ Microbiol 2005;71:8970–3. https://doi.org/10.1128/AEM.71.12.8970-8973.2005.

[30] Nakayama K, Takashima K, Ishihara H, Shinomiya T, Kageyama M, Kanaya S, et al. The R-type pyocin of *Pseudomonas aeruginosa* is related to P2 phage, and the F-type is related to lambda phage. Mol Microbiol 2000;38:213–31. https://doi.org/10.1046/j.1365-2958.2000.02135.x.

[31] Jacob F. [Induced biosynthesis and mode of action of a pyocine, antibiotic produced by *Pseudomonas aeruginosa*]. Ann Inst Pasteur (Paris) 1954;86:149–60.

[32] Uratani Y, Hoshino T. Pyocin R1 inhibits active transport in *Pseudomonas aeruginosa* and depolarizes membrane potential. J Bacteriol 1984;157:632–6. https://doi.org/10.1128/jb.157.2.632-636.1984.

[33] Aldová E, Hausner O, Kocmoud Z, Schindler J, Petrás P. A new member of the family *Enterobacteriaceae-Pragia fontium*. J Hyg Epidemiol Microbiol Immunol 1988;32:433–6.

[34] Aldová E, Hausner O, Gabrhelová M. *Budvicia*-a new genus of *Enterobacteriaceae*. Data on phenotypic characters. J Hyg Epidemiol Microbiol Immunol 1984;28: 234–7.

[35] Baek C, Shin S-K, Yi H. *Limnobaculum parvum* gen. nov., sp. nov., isolated from a freshwater lake. Int J Syst Evol Microbiol 2019;69:1826–30. https://doi.org/10.1099/ijsem.0.003401.

[36] Lang E, Schumann P, Knapp BA, Kumar R, Spröer C, Insam H. *Budvicia diplopodorum* sp. nov. and emended description of the genus *Budvicia*. Int J Syst Evol Microbiol 2013;63:260–7. https://doi.org/10.1099/ijs.0.036749-0.

[37] Lee SD, Byeon Y-S, Kim S-M, Yang HL, Kim IS. *Jinshanibacter allomyrinae* sp. nov., isolated from larvae of *Allomyrina dichotoma*, proposal of *Insectihabitans xujianqingii*

gen. nov., comb. nov. and emended descriptions of the genera *Jinshanibacter, Limnobaculum* and *Pragia*. Int J Syst Evol Microbiol 2021;71. https://doi.org/10.1099/ijsem.0.004938.

[38] Li N-N, Wang H-C, Li J-Y, He W, Xue H-P, Gao T-H, et al. Description of *Limnobaculum eriocheiris* sp. nov., an intestinal bacterium of *Eriocheir sinensis*, and reclassification of the genera *Jinshanibacter* and *Insectihabitans* as *Limnobaculum*. Antonie Leeuwenhoek 2023;116:487–97. https://doi.org/10.1007/s10482-023-01819-y.

[39] Ge Y, Wang B, Yang J, Lai X-H, Zhang G, Lu S, et al. *Jinshanibacter*, a new genus of *Budviciaceae*: identification of *Jinshanibacter zhutongyuii* sp. nov. and *Jinshanibacter xujianqingii* sp. nov. isolated from cloacal content of snow finch (*Montifringilla taczanowskii*). Int J Syst Evol Microbiol 2021;71. https://doi.org/10.1099/ijsem.0.004653.

[40] Hickman-Brenner FW, Vohra MP, Huntley-Carter GP, Fanning GR, Lowery VA, Brenner DJ, et al. *Leminorella*, a new genus of *Enterobacteriaceae*: identification of *Leminorella grimontii* sp. nov. and *Leminorella richardii* sp. nov. found in clinical specimens. J Clin Microbiol 1985;21:234–9. https://doi.org/10.1128/jcm.21.2.234-239.1985.

[41] Smarda J. Production of bacteriocin-like agents of *Budvicia aquatica* and "*Pragia fontium*.". Zentralbl Bakteriol Mikrobiol Hyg 1987;265:74–81.

[42] Látrová K, Dolejšová T, Motlová L, Mikušová G, Bosák J, Snopková K, Šmajs D, Konopásek I, Fišer R. R-type fonticins produced by *Pragia fontium* form large pores with high conductance. J Bacteriol 2023;205:e0031522. https://doi.org/10.1128/jb.00315-22.

[43] Snopkova K, Dufkova K, Klimesova P, Vanerkova M, Ruzicka F, Hola V. Prevalence of bacteriocins and their co-association with virulence factors within *Pseudomonas aeruginosa* catheter isolates. Int J Med Microbiol 2020;310:151454. https://doi.org/10.1016/j.ijmm.2020.151454.

[44] Arndt D, Grant JR, Marcu A, Sajed T, Pon A, Liang Y, et al. PHASTER: a better, faster version of the PHAST phage search tool. Nucleic Acids Res 2016;44:W16–21. https://doi.org/10.1093/nar/gkw387.

[45] Rodriguez-R LM, Konstantinidis KT. The enveomics collection: a toolbox for specialized analyses of microbial genomes and metagenomes. PeerJ Inc.; 2016. https://doi.org/10.7287/peerj.preprints.1900v1.

[46] Rossignol M, Basset A, Espéli O, Boccard F. NKBOR, a mini-Tn10-based transposon for random insertion in the chromosome of Gram-negative bacteria and the rapid recovery of sequences flanking the insertion sites in *Escherichia coli*. Res Microbiol 2001;152:481–5. https://doi.org/10.1016/S0923-2508(01)01221-9.

[47] Bosák J, Laiblová P, Smarda J, Dedicová D, Smajs D. Novel colicin Fy of *Yersinia frederiksenii* inhibits pathogenic *Yersinia* strains via YiuR-mediated reception, TonB import, and cell membrane pore formation. J Bacteriol 2012;194:1950–9. https://doi.org/10.1128/JB.05885-11.

[48] Green MR, Sambrook J, Sambrook J. Molecular cloning: a laboratory manual. In: Cold spring harbor. fourth ed. N.Y: Cold Spring Harbor Laboratory Press; 2012.

[49] Grinter R, Milner J, Walker D. Bacteriocins active against plant pathogenic bacteria. Biochem Soc Trans 2012;40:1498–502. https://doi.org/10.1042/BST20120206.

[50] Mojesky AA, Remold SK. Spatial structure maintains diversity of pyocin inhibition in household *Pseudomonas aeruginosa*. Proc Biol Sci 2020;287:20201706. https://doi.org/10.1098/rspb.2020.1706.

[51] Scholl D, Cooley M, Williams SR, Gebhart D, Martin D, Bates A, et al. An engineered R-type pyocin is a highly specific and sensitive bactericidal agent for the food-borne pathogen *Escherichia coli* O157:H7. Antimicrob Agents Chemother 2009;53:3074–80. https://doi.org/10.1128/AAC.01660-08.

[52] Bhattacharjee R, Nandi A, Sinha A, Kumar H, Mitra D, Mojumdar A, et al. Phage-tail-like bacteriocins as a biomedical platform to counter anti-microbial resistant pathogens. Biomed Pharmacother 2022;155:113720. https://doi.org/10.1016/j.biopha.2022.113720.

[53] Dorosky RJ, Yu JM, Pierson LS, Pierson EA. *Pseudomonas chlororaphis* produces two distinct R-tailocins that contribute to bacterial competition in biofilms and on roots. Appl Environ Microbiol 2017;83. https://doi.org/10.1128/AEM.00706-17.

[54] Fernandez M, Godino A, Príncipe A, López Ramírez V, Quesada JM, Rigo V, et al. Characterization of the bacteriocins and the PrtR regulator in a plant-associated *Pseudomonas* strain. J Biotechnol 2020;307:182–92. https://doi.org/10.1016/j.jbiotec.2019.11.003.

[55] Ghequire MGK, Dillen Y, Lambrichts I, Proost P, Wattiez R, De Mot R. Different ancestries of R tailocins in rhizospheric *Pseudomonas* isolates. Genome Biol Evol 2015;7:2810–28. https://doi.org/10.1093/gbe/evv184.

[56] Yao GW, Duarte I, Le TT, Carmody L, LiPuma JJ, Young R, et al. A broad-host-range tailocin from *Burkholderia cenocepacia*. Appl Environ Microbiol 2017;83: e03414. https://doi.org/10.1128/AEM.03414-16. 16.

[57] Nguyen HA, Tomita T, Hirota M, Kaneko J, Hayashi T, Kamio Y. DNA inversion in the tail fiber gene alters the host range specificity of carotovoricin Er, a phage-tail-like bacteriocin of phytopathogenic *Erwinia carotovora* subsp. carotovora Er. J Bacteriol 2001;183:6274–81. https://doi.org/10.1128/JB.183.21.6274-6281.2001.

[58] Yamada K, Hirota M, Niimi Y, Nguyen HA, Takahara Y, Kamio Y, et al. Nucleotide sequences and organization of the genes for carotovoricin (Ctv) from *Erwinia carotovora* indicate that Ctv evolved from the same ancestor as *Salmonella typhi* prophage. Biosci Biotechnol Biochem 2006;70:2236–47. https://doi.org/10.1271/bbb.60177.

[59] Vacheron J, Heiman CM, Keel C. Live cell dynamics of production, explosive release and killing activity of phage tail-like weapons for *Pseudomonas* kin exclusion. Commun Biol 2021;4:1–14. https://doi.org/10.1038/s42003-020-01581-1.

[60] Abuladze NK, Gingery M, Tsai J, Eiserling FA. Tail length determination in bacteriophage T4. Virology 1994;199:301–10. https://doi.org/10.1006/viro.1994.1128.

[61] Katsura I, Hendrix RW. Length determination in bacteriophage lambda tails. Cell 1984;39:691–8. https://doi.org/10.1016/0092-8674(84)90476-8.

[62] Agrain C, Callebaut I, Journet L, Sorg I, Paroz C, Mota LJ, et al. Characterization of a Type III secretion substrate specificity switch (T3S4) domain in YscP from *Yersinia enterocolitica*: characterization of a T3S4 domain in YscP. Mol Microbiol 2005;56:54–67. https://doi.org/10.1111/j.1365-2958.2005.04534.x.

[63] Cornelis GR. The type III secretion injectisome. Nat Rev Microbiol 2006;4:811–25. https://doi.org/10.1038/nrmicro1526.

[64] Rybakova D, Schramm P, Mitra AK, Hurst MRH. Afp14 is involved in regulating the length of Anti-feeding prophage (Afp). Mol Microbiol 2015;96:815–26. https://doi.org/10.1111/mmi.12974.

[65] Fischer S, Godino A, Quesada JM, Cordero P, Jofré E, Mori G, et al. Characterization of a phage-like pyocin from the plant growth-promoting rhizobacterium *Pseudomonas fluorescens* SF4c. Microbiology (Reading) 2012;158: 1493–503. https://doi.org/10.1099/mic.0.056002-0.

[66] Hockett KL, Renner T, Baltrus DA. Independent Co-option of a tailed bacteriophage into a killing complex in Pseudomonas, vol. 6; 2015. p. 11.